Full Articles

Crystal structure and properties of the $Na_{1-x}Ru_2O_4$ phase

R. V. Panin,[a]★ N. R. Khasanova,[a] A. M. Abakumov,[a,b] W. Schnelle,[c] J. Hadermann,[b] and E. V. Antipov[a]

[a]*Department of Chemistry, M. V. Lomonosov Moscow State University, 1 Leninskie Gory, 119992 Moscow, Russian Federation. Fax: +7 (495) 939 4788. E-mail: panin@icr.chem.msu.ru*
[b]*EMAT University of Antwerp (RUCA), 171 Groenenborgerlaan, 2020 Antwerp, Belgium*
[c]*Max-Planck Institute of Chemical Solid State Physics (CPfS), 40 Nöthnitzer, 01187 Dresden, Germany*

Sodium ruthenium(III,IV) oxide $Na_{1-x}Ru_2O_4$ was synthesized by the solid state reaction of Na_2CO_3 and RuO_2 in inert atmosphere and characterized by X-ray powder diffraction, electron diffraction, and high-resolution transmission electron microscopy. The compound crystallizes in the $CaFe_2O_4$-type structure (space group *Pnma*, $Z = 4$, $a = 9.2641(7)$ Å, $b = 2.8249(3)$ Å, $c = 11.1496(7)$ Å). Double rutile-like chains of the RuO_6 octahedra form a three-dimensional framework, whose tunnels contain sodium cations. The structure contains two crystallographically independent sites of ruthenium atoms randomly occupied by the Ru^{III} and Ru^{IV} cations. The superstructure with the doubled *b* parameter found for one of the samples under study using electron diffraction is caused, probably, by ordering of the Ru cations in the rutile-like chains. The $Na_{1-x}Ru_2O_4$ compound exhibits temperature-independent paramagnetism with $\chi_0 = 1.9 \cdot 10^{-4}$ cm^3 (mole of Ru^{-1}).

Key words: sodium ruthenium(III,IV) oxide, double rutile-like chains, $CaFe_2O_4$-type structure, superstructure with doubling of *b* parameter, sodium nonstoichiometry.

In the recent time, complex ruthenium oxides are under intense studies, which is explained by the poorly known chemistry of ruthenates and increasing interest in the nature and character of magnetic interactions in these compounds. Diversity of complex ruthenium oxides is caused by the ability of ruthenium cations to form different coordination polyhedra, depending on the oxidation state. These polyhedra link to each other in different manners to form layered, framework, and chain structures. Almost all types of combination of ruthenium—oxygen polyhedra are observed in the Na—Ru—O system. The "ruthenium bronze" $Na_{3-x}Ru_4O_9$ and Na_3RuO_4 phase[1—3] are tunneling structures formed due to linking the RuO_6 octahedra through the common edges and vertices. Paramagnetic $NaRuO_2$ is isostructural to α-$NaFeO_2$ and contains hexagonal octahedral RuO_2 layers.[4] Isolated chains of trigonal

Published in Russian in *Izvestiya Akademii Nauk. Seriya Khimicheskaya,* No. 10, pp. 1655—1660, October, 2006.
1066-5285/06/5510-1717

bipyramids (RuO_5) linked through the opposite vertices form the structure of Na_2RuO_4 that exhibits the antiferromagnetic transition below 37 K.[5] The synthesis of one more phase in the Na—Ru—O ($NaRu_2O_4$) system has been reported earlier[6]; however, no detailed information on the structure and physical properties of this compound was given. In the present work we describe the synthesis, crystal structure, and magnetic properties of the $Na_{1-x}Ru_2O_4$ phase. The obtained results are discussed and compared with available data and the results published[7] when the present article was prepared for publication.

Experimental

Compound $Na_{1-x}Ru_2O_4$ was synthesized by the solid state reaction of Na_2CO_3 (99.99%) and RuO_2 (99.9%) pre-calcined at 500 and 700 °C, respectively. The initial reagents were stirred under acetone, pressed in pellets, and annealed in a high-purity argon flow.

X-ray powder diffraction data for the crystal structure refinement were obtained using a Huber X-ray chamber (Image Plate, G670 detector, Cu-Kα1 radiation, germanium monochromator, transmission regime). Full-profile refinement of the crystal structure by the Rietveld method was performed using the JANA2000 program.[8] The bond valence sums were calculated according to the Brown—Altermatt formula,[9] and the r_o constants for ruthenium were borrowed from Ref. 10.

X-ray local spectral analysis (XLSA) was carried out on a Supra 50VP scanning electron microscope (LEO Carl Zeiss, Germany) equipped with an INCA spectrometer (Oxford, England). Intensities of the K-line of Na and L-line of Ru were used for quantitative determination of sodium and ruthenium. Electron diffraction patterns were obtained on a Philips CM20 transmission electron microscope. Samples were deposited on a copper grid covered with a thin amorphous perforated carbon film. High-resolution images were obtained on a JEOL 4000EX electron microscope, and simulated images were retrieved using the MacTempas program package.

Magnetic measurements were carried out on a Quantum Design SQUID magnetometer in the temperature interval from 1.8 to 400 K at $H = 0.01$—7 T.

Results and Discussion

Attempts to prepare $Na_{1-x}Ru_2O_4$ in quartz ampules under described conditions[6] were unsuccessful and, hence, the synthesis was further conducted in a high-purity argon flow. Sodium losses occurred during the synthesis influenced the phase composition of the samples and, therefore, several parameters were optimized to prepare a single-phase sample: molar ratio of the initial reagents, heating regime, annealing temperature, and annealing time.

The molar ratio $Na_2CO_3 : RuO_2 = 1 : 1$ was found to be optimal. High content of carbonate in the initial mixture resulted in the predominant formation of $NaRuO_2$ or melting of the reaction mixture to form poorly crystallized products, whereas at a lower Na_2CO_3 content considerable amounts of the initial RuO_2 remained unreacted. Preliminary experiments showed that the initial reagents begin to interact at temperatures above 850 °C and the optimum temperature is ~950 °C. Nevertheless, at these temperatures the synthesis remained poorly reproducible and resulted in different phases. For example, annealing for 7 h at 950 °C gave "ruthenium bronze" $Na_{3-x}Ru_4O_9$ as the major product. An increase in the annealing time to 10 h resulted in the formation of $Na_{1-x}Ru_2O_4$ and $NaRuO_2$ in the approximately equal molar ratio, and only the lines of RuO_2 were observed in the X-ray pattern when the annealing time increased to 24 h. The results of phase analysis of several samples obtained under different conditions and containing $Na_{1-x}Ru_2O_4$ are presented in Table 1. Taking into account these peculiarities, the two-stage procedure was proposed for the preparation of pure $Na_{1-x}Ru_2O_4$. At the first stage the initial components were annealed at 950 °C for a more complete interaction of the initial reagents, and then the temperature was increased to 1030 °C, which resulted in partial sodium removal and predominant formation of $Na_{1-x}Ru_2O_4$. At each stage the annealing time was optimized until the content of impurity phases in the sample decreased to 1—3%. As a result, the following temperature regime was proposed:

Table 1. Phase analysis of samples *1*—*5* synthesized under different conditions

Sample	Initial composition	T*/°C	t**/h	Unit cell parameters/Å			V/Å^3	Impurity phases (I_{max} (%))
				a	*b*	*c*		
1	$Na_2CO_3 : RuO_2 = 2 : 1$	950	10	9.2732(8)	2.8237(3)	11.1637(8)	292.32(2)	$NaRuO_2$ (15)
2	$Na_2CO_3 : RuO_2 = 2 : 1$	1010	5	9.268(2)	2.8198(5)	11.161(1)	291.69(1)	$NaRuO_2$ (7—10)
3	$Na_2CO_3 : RuO_2 = 1 : 1$	950	5	9.267(3)	2.828(1)	11.152(4)	292.20(3)	$Na_{3-x}Ru_4O_9$ (8)
		1020	5					
4	$Na_2CO_3 : RuO_2 = 1 : 1$	950	10	9.2641(7)	2.8249(3)	11.1496(7)	291.79(3)	RuO_2 (2)
		1030	5					
5	$Na_2CO_3 : RuO_2 = 2 : 1$	1015	10	9.263(1)	2.8296(4)	11.135(1)	291.85(3)	RuO_2 (5)

* Annealing temperature.

** Annealing time at the indicated temperature.

25—950 °C (170 °C h^{-1}), 950 °C (5 h), 950—1030 °C (170 °C h^{-1}), and 1030 °C (5 h) followed by cooling to room temperature in the cooling down oven.

The X-ray pattern of a dark gray powder prepared according to the above procedure (sample *4*) was indexed in the orthorhombic crystal system (space group *Pnma*) with the unit cell parameters a = 9.2641(7) Å, b = 2.8249(3) Å, and c = 11.1496(7) Å, which agree well with the previously published values.[6] According to the XLSA data, the cationic Na : Ru ratio for this sample is 34.0(6) : 66.0(5), *i.e.*, close to 1 : 2. It should be mentioned that the unit cell parameters of the phase under study differ for the samples synthesized under different conditions (see Table 1). This can be due to cationic nonstoichiometry of $Na_{1-x}Ru_2O_4$ (see below).

The crystal structure of $Na_{1-x}Ru_2O_4$ was refined by the powder diffraction data for sample *4*. Detailed analysis of the X-ray pattern revealed the presence of a small amount of the RuO_2 impurity phase, which was included in the refinement using published structural data.[11] The unit cell parameters and scale factor were refined for RuO_2. According to full-matrix analysis, the content of RuO_2 was 2 wt.%. The $Na_{1-x}Ru_2O_4$ structure was refined in the space group *Pnma*, and the data for the $CaFe_2O_4$ structure were used as the initial model.[12] The atomic displacement parameters were refined in the isotropic approximation, and refinement for the oxygen atoms was carried out using the general parameter of atomic displacement. The refinement of the site occupancy for Na gave the formula $Na_{0.94}Ru_2O_4$. As a result, the reasonable structure parameters and good coincidence between the observed and calculated profiles were obtained (R_{wp} = 0.0187, R_p = 0.0134, R_I = 0.0513). The diffraction pattern of the sample and difference curve between the observed and calculated profiles are shown in Fig. 1. The atomic coordinates and atomic displacement parameters are presented in Table 2. Selected interatomic distances are given in Table 3.

Table 2. Atomic coordinates (x, y, and z) and atomic displacement parameters (U_{iso}) for the $Na_{1-x}Ru_2O_4$ structure

Atom	Site	Site occupancy	x/a	y/b	z/c	U_{iso}/Å^2
Na	4c	0.94(1)	0.7218(7)	1/4	0.6591(6)	0.043(2)
Ru(1)	4c	1.0	0.4432(1)	1/4	0.6134(1)	0.0216(7)
Ru(2)	4c	1.0	0.4145(1)	1/4	0.1038(1)	0.0186(6)
O(1)	4c	1.0	0.2084(5)	1/4	0.1555(7)	0.025(1)
O(2)	4c	1.0	0.101(1)	1/4	0.4786(5)	0.025(1)
O(3)	4c	1.0	0.512(1)	1/4	0.7804(5)	0.025(1)
O(4)	4c	1.0	0.4114(7)	1/4	0.4266(6)	0.025(1)

Table 3. Selected interatomic distances (r) in the $Na_{1-x}Ru_2O_4$ structure

Distance	r/Å	Distance	r/Å
Ru(1)—O(1)	2×2.047(4)	Ru(2)—O(3)	2×2.029(4)
Ru(1)—O(3)	1.969(5)	Na—O(1)	2×2.506(9)
Ru(1)—O(4)	2×2.002(5)	Na—O(2)	2×2.367(7)
Ru(1)—O(4)	2.101(7)	Na—O(3)	2.273(11)
Ru(2)—O(1)	1.995(5)	Na—O(3)	2.809(10)
Ru(2)—O(2)	2×1.991(3)	Na—O(4)	2×2.448(8)
Ru(2)—O(2)	1.957(8)		

According to the refinement results, the phase under study is isostructural to $CaFe_2O_4$. The RuO_6 octahedra are linked through the common edges to form double rutile-like chains, which are connected through the common vertices and form a three-dimensional framework, whose tunnels contain the Na atoms (Fig. 2). The structure has two crystallographic sites of the ruthenium at-

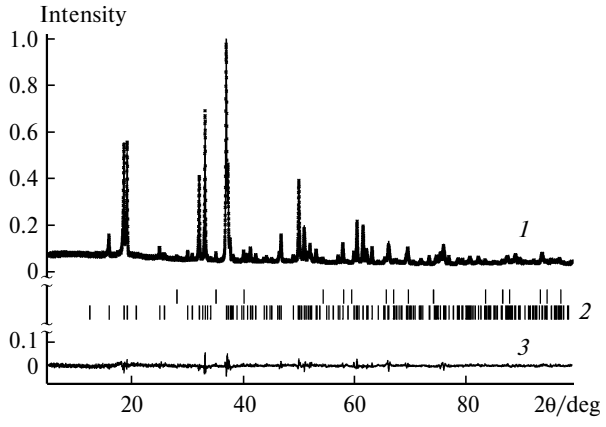

Fig. 1. Full-profile refinement of the $Na_{1-x}Ru_2O_4$ crystal structure: diffraction pattern of the sample (*1*), calculated sites of reflections for the $Na_{1-x}Ru_2O_4$ (*2*, bottom) and RuO_2 (*2*, top) phases and the difference curve of the observed and calculated profiles (*3*).

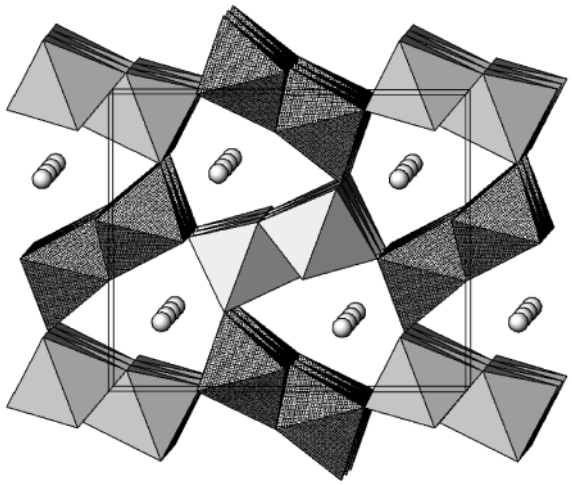

Fig. 2. Projection of the $Na_{1-x}Ru_2O_4$ crystal along the [010] direction. Octahedra $Ru(1)O_6$ and $Ru(2)O_6$ are differently colored, and the sodium atoms are presented as spheres.

oms, and each chain contains ruthenium atoms of the same type. The RuO_6 octahedra are slightly distorted, and the Ru—O distances are in the 1.97—2.10 and 1.96—2.03 Å ranges for Ru(1) and Ru(2), respectively. The Ru—Ru distances in the chain are 2.83 and ~3.1 Å, whereas the shortest Ru(1)—Ru(2) distance between the atoms in the adjacent chains is much longer, being 3.6 Å. The sodium atom is coordinated to eight oxygen atoms, and a two-capped trigonal prism is the coordination polyhedron of sodium. The Na—O distance ranges from 2.37 to 2.58 Å. The site occupancy of Na deviates slightly from 1 and, hence, the ruthenium sublattice in $Na_{1-x}Ru_2O_4$ contains approximately equal amounts of the Ru^{III} and Ru^{IV} atoms. According to the calculation of the bond valence sums, the formal oxidation states of ruthenium for the Ru(1) and Ru(2) sites are equal to 3.4 and 3.5, respectively.

Partial occupancy of the cationic site in the tunnels is characteristic of hollandite-like structures, and such compounds are also known among those crystallizing in the $CaFe_2O_4$-type structure, for instance, $Na_{0.7}(FeAl)_{0.7}Ti_{1.3}O_4$.[13] In the case of sodium ruthenium(III,IV) oxide, the deviation from the sodium stoichiometric composition is small; nevertheless, the change in the unit cell parameters for the samples synthesized under different conditions (see Table 1) shows that the formation of $Na_{1-x}Ru_2O_4$ with different site occupancies of Na cannot be excluded.

The electron diffraction study of sample *3* showed the presence of a superstructure. The main reflections in the electron diffraction patterns were indexed in the orthorhombic cell with the parameters $a \approx 9.26$ Å, $b \approx 2.83$ Å, and $c \approx 11.15$ Å; however, superstructure reflections corresponding to doubling of the *b* parameter are observed in the patterns for the [100]*, [001]*, [140]*, and [041]* zones (Fig. 3). The only reflection condition that can be determined from the electron diffraction patterns is $hk0$, $h = 2n$ for the [001]* zone, which corresponds to the diffraction symbol $P\_\ \_a$. The presence of the reflections $h00$, $h \neq 2n$ in the patterns for the [010]*, [012]*, and [021]* zones is due to double diffraction, which is confirmed by the absence of these reflections from the electron diffraction pattern for the [001]* zone. Based on the analysis of the obtained diffraction patterns and taking into account specific features of the $Na_{1-x}Ru_2O_4$ structure, we proposed the space groups $P112_1/a$ and $P11a$ with the indicated transition matrix.

$$\begin{pmatrix} 1 & 0 & 0 \\ 0 & 2 & 0 \\ 0 & 0 & 1 \end{pmatrix}$$

For the centrosymmetric group $P11a$, the origin should be shifted by (0 1/8 1/4). However, full-matrix refinement with account for the superstructure is impossible, because no additional superstructure reflections were observed in the X-ray pattern.

High-resolution images for the [001] and [100] zones were used to reveal the origin of the observed superstructure. The images of the [001] zones were calculated using structural data obtained by refinement. The best correspondence between the experimental and calculated images (Fig. 4, *a*) was achieved at the defocus value

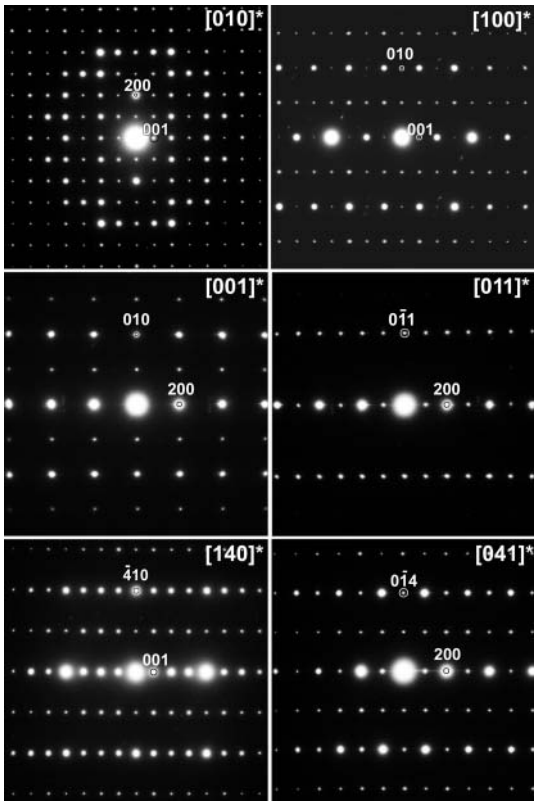

Fig. 3. Electron diffraction patterns of different zones for $Na_{1-x}Ru_2O_4$. Indexing was performed with the sublattice parameters.

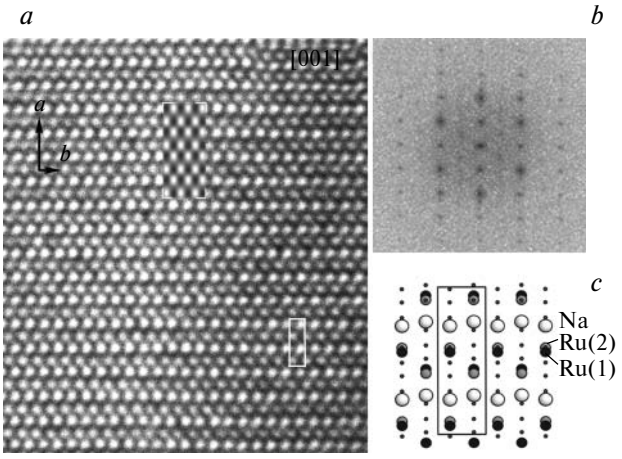

Fig. 4. *a*. High-resolution image for the [001] zone (simulated image obtained at $\Delta f = +50$ Å and $t = 15$ Å is shown in inset). *b*. Fourier transformation of the image confirming validity of indexing of the presented plane. *c*. Projection of the $Na_{1-x}Ru_2O_4$ structure along the *c* axis.

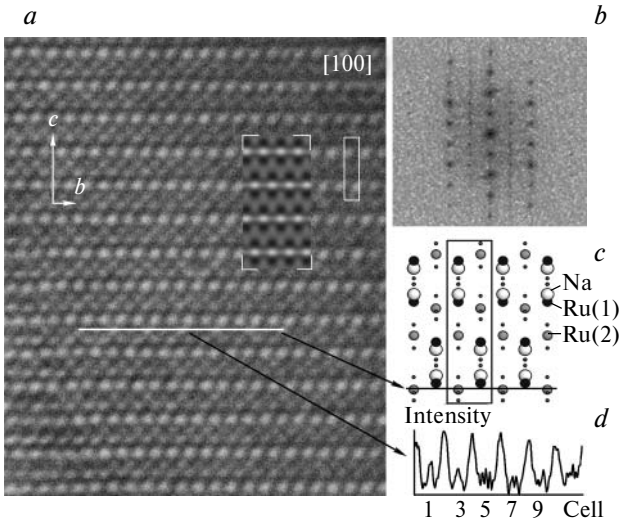

Fig. 5. *a*. High-resolution image for the [100] zone (simulated image obtained at $\Delta f = -185$ Å and $t = 20$ Å is shown in inset). *b*. Fourier transformation of the image confirming validity of indexing of the presented zone. *c*. Projection of the $Na_{1-x}Ru_2O_4$ structure along the *a* axis. *d*. Intensity distribution of the Ru(2) atoms in the column along the *b* axis.

$\Delta f = +50$ Å and crystallite thickness $t = 15$ Å. Reasons for the appearance of the superstructure for this zone is not so obvious, which is confirmed by the diffuse character of the superstructure reflections for the reciprocal Fourier transform (Fig. 4, *b*). For this zone, only the Na atoms form particular columns, whereas the Ru(1) and Ru(2) atoms are projected onto each other (Fig. 4, *c*). Therefore, it can be assumed that the appearance of the superstructure is not related to ordering of the Na cations and vacancies along the tunnels arranged *via* the *b* axis. The image along the *a* axis ([100] zone) presented in Fig. 5 is most informative. For this direction, the columns of metal atoms of different types are not projected onto each other, which makes it possible to separate the contribution of atoms of each type (see Fig. 5, *c*). Simulation of the images using the refined structure model ($\Delta f = -185$ Å, $t = 20$ Å) revealed the correspondence between the intensity distribution on the image and fragments of the $Na_{1-x}Ru_2O_4$ structure. The arrays of bright spots were found to correspond to the columns of the Ru(1) and Na atoms, whereas the zigzag arrays of the lower-intensity spots between them belong to the columns of the Ru(2) atoms. The intensity distribution of the spots corresponding to the columns of Ru(2) along the *b* axis (see Fig. 5, *d*) is nonuniform: every second spot has lower intensity. This suggests a different coordination environment of the Ru(2) atoms in the rutile-like chain and, hence, possible charge ordering of the ruthenium cations.

To confirm this hypothesis, additional neutron diffraction studies are necessary. Nevertheless, no superstructure caused by ordering of Ru cations was found in

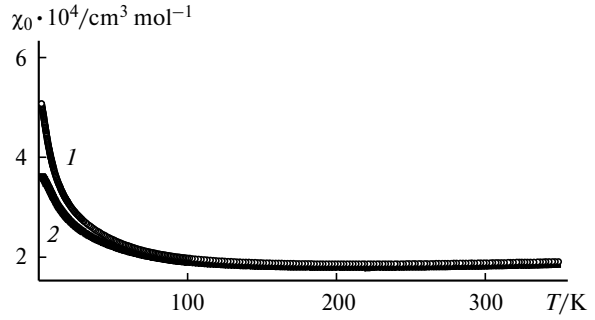

Fig. 6. Temperature dependence of the magnetic susceptibility of $Na_{1-x}Ru_2O_4$ (χ_0) at $H = 3.5$ (*1*) and 7 T (*2*).

Ref. 7, where the structure was determined by neutron powder diffraction data. It can be assumed that this is due to nonstoichiometry of $Na_{1-x}Ru_2O_4$; as a result, ordering of the ruthenium cations occurs only at a certain composition of $Na_{1-x}Ru_2O_4$. Variation of the cell parameters observed for the samples synthesized under different conditions and the results of structure refinement[7] agree with this assumption.

Magnetic measurements for sample *4* containing insignificant amounts of RuO_2 were carried out in different magnetic fields and corrected to the presence of this impurity (Fig. 6). The measurements showed no phase transitions in the temperature interval from 1.8 to 400 K and in fields with 7 T > H > 0.01 T. In the 100—400 K interval, $Na_{1-x}Ru_2O_4$ is a temperature-independent paramagnetic ($\chi_0 \approx 1.9 \cdot 10^{-4}$ cm^3 (mole of Ru)$^{-1}$). The magnetic susceptibility increases at lower temperatures. The obtained χ/T dependence agrees well with published data[7]; nevertheless, the authors of Ref. 7 describe the $Na_{1-x}Ru_2O_4$ compound as a temperature-independent paramagnetic in the whole temperature interval, and the increase in the magnetic susceptibility observed at low temperatures is explained by an insignificant amount of an unknown paramagnetic impurity. Similar magnetic behavior is also observed in the $Na_{1-x}Ca_xRh_2O_4$ system on going from $NaRh_2O_4$ characterized as the Pauli paramagnetic to the $CaRh_2O_4$ phase.[14] In this case, the increase in χ at low temperatures is interpreted as paramagnetism caused by localized magnetic moments. Additional measurements of samples with different stoichiometry are required for the final elucidation of this magnetic behavior.

The $CaFe_2O_4$-type structure is rather abundant for compounds with the AB_2O_4 composition.[15] This type is observed for compounds containing cations A and B in the eightfold and sixfold oxygen environment at a certain ratio between the radii of these cations (r_A/r_B). The r_A/r_B value is varied in a wide range: from 1.3 ($CaYb_2O_4$) to 2.2 ($NaAlGeO_4$).[16,17] If the ratio $r_A/r_B > 2.3$, then compounds of another composition differed from AB_2O_4 are formed. The fact that $Na_{1-x}Ru_2O_4$ ($r_A/r_B \approx 1.78$) crystallizes in the $CaFe_2O_4$-type structure agrees well with the

above formulated criteria. This structural type should be observed for the $CaRu_2O_4$ phase ($r_A/r_B \approx 1.64$) if it will be prepared.

In almost all $NaM^{III}M^{IV}O_4$ compounds (M = Fe, Ti, Sn, Rh) that crystallize in the $CaFe_2O_4$-type structure, the M^{III} and M^{IV} cations are randomly distributed over two octahedral sites, which slightly differ from each other. Cation ordering is observed in the $NaMn_2O_4$ compound synthesized recently[18] under high pressure. The presence of the Mn^{III} atom prone to the Jahn—Teller distortion results in structural rearrangement and realization of two different octahedral sites, due to which each rutile-like chain contains either Mn^{III} or Mn^{IV}. Ordering of the Ru cations found for sample *3* is different: it occurs in rutile-like chains and produces a superstructure. However, since the Ru^{IV} atom has the electron configuration d^4 similar to that of Mn^{III}, we cannot rule out the participation of the Jahn—Teller distortion in the appearance of the superstructure for $Na_{1-x}Ru_2O_4$ as well.

The authors are grateful to A. V. Knot´ko and A. V. Garshev for performing X-ray local spectral analysis and to Yu. A. Velikodnyi for X-ray experiments.

References

1. J. Darriet, *Acta Crystallogr., Sect. B*, 1974, **30**, 1459.
2. J. Darriet and J. Galy, *Bull. Soc. Fr. Mineral. Cristallogr.*, 1974, **97**, 3.
3. K. A. Regan, Q. Huang, and R. J. Cava, *J. Solid State Chem.*, 2005, **178**, 2104.
4. M. Shikano, C. Delmas, and J. Darriet, *Inorg. Chem.*, 2004, **43**, 1214.
5. M. Shikano, R. K. Kremer, M. Ahrens, H.-J. Koo, M.-H. Whangbo, and J. Darriet, *Inorg. Chem.*, 2004, **43**, 5.
6. J. Darriet, *Bull. Soc. Fr. Mineralog. Cristallogr.*, 1975, **98**, 374.
7. K. A. Regan, Q. Huang, M. Lee, A. P. Ramirez, and R. J. Cava, *J. Solid State Chem.*, 2005, **179**, 195.
8. V. Petricek and M. Dusek, *JANA2000: Programs for Modulated and Composite Crystals*, Institute of Physica, Praha (Czech Republic), 2000.
9. I. D. Brown and D. Altermatt, *Acta Crystallogr.*, *Sect B*, 1985, **41**, 244.
10. N. E. Brese and M. O´Keeffe, *Acta Crystallogr.*, *Sect. B*, 1991, **47**, 192.
11. A. A. Bolzan, C. Fong, B. J. Kennedy, and C. J. Howard, *Acta Crystallogr.*, *Sect. B*, 1997, **53**, 373.
12. D. F. Becker and J. S. Kasper, *Acta Crystallogr.*, 1957, **10**, 332.
13. H. Mueller-Buschbaum and D. Frerichs, *J. Alloys Comp.*, 1993, **199**, 8.
14. K. Yamaura, Q. Huang, M. Moldovan, D. P. Young, A. Sato, Y. Baba, Y. Matsui, and E. Takayama-Muromachi, *Chem. Mater.*, 2005, **17**, 359.
15. H. Mueller-Buschbaum, *J. Alloys Comp.*, 2003, **349**, 49.
16. H. Mueller-Buschbaum and R. von Schenk, *Z. Anorg. Allg. Chem.*, 1970, **377**, 70.
17. A. F. Reid, A. D. Wadsley, and M. J. Sienko, *Inorg. Chem.*, 1968, **7**, 112.
18. J. Akimoto, J. Awaka, N. Kijima, Y. Takahashi, Y. Maruta, K. Tokiwa, and T. Watanabe, *J. Solid State Chem.*, 2006, **179**, 169.

Received June 2, 2006;
in revised form September 19, 2006